

Supporting Information

Interaction between Palladium-Doped Zerovalent Iron Nanoparticles and Biofilm in Granular Porous Media: Characterization, Transport and Viability

MOHAN BASNET¹, ALEXANDER GERSHANOV¹, KEVIN J. WILKINSON², SUBHASIS GHOSHAL³, and NATHALIE TUFENKJI^{*, 1}

¹Department of Chemical Engineering, McGill University, Montreal, Quebec H3A 0C5, Canada

²Department of Chemistry, University of Montreal, Montreal, Quebec H3C 3J7, Canada

³Department of Civil Engineering, McGill University, Montreal, Quebec H3A 0C3, Canada

* Corresponding Author. Phone: (514) 398-2999; Fax: (514) 398-6678; E-mail: nathalie.tufenkji@mcgill.ca

Table S1. Summary of nanoparticle transport studies conducted using columns packed with biofilm-coated granular materials.

particles	column parameters			biofilm type	biofilm growth method	solution chemistry	approach velocity	major findings and conclusions	references
	grain	porosity	length						
RL-coated and CMC-coated Pd-NZVI	quartz sand (256 μm)	0.37	8.1 cm	<i>Pseudomonas aeruginosa</i> PAO1	batch culture with sand in a shaking incubator at 37°C for 24 h	1-100 mM NaCl and 1-30 mM CaCl_2 (pH 7.7)	7.5×10^{-5} m/s	increased nanoparticle retention in the presence of biofilm; straining was an important retention mechanism for an aggregated suspension	this study
PVP-stabilized nAg	quartz sand (760 μm)	0.37	8 cm	<i>Pseudomonas aeruginosa</i> PAO1	batch culture with sand in a shaking incubator at 35 \pm 2 °C for 24-96 h	1-100 mM NaNO_3 and 1-100 mM CaNO_3 (pH 7)	6.2×10^{-5} m/s	decreased nanoparticle retention in biofilm-coated sand compared to clean sand; repulsive electrosteric interaction between PVP coating and bacterial extracellular polymeric substances (EPS) was likely a governing mechanism	Mitzel and Tufenkji, 2014
ZnO, CeO_2 , TiO_2 and Ag nanoparticles	used/fresh filter sand (500 μm) and treated sand (700 μm)	0.34	15 cm	mixed culture	biofilm in drinking water sand filter (consisting of bacteria, bacteriophages and protozoa)	(pH 7.2)	N/A	increased nanoparticle retention in the presence of biofilm, however to a lesser extent for capped nanoparticles	Li et al. 2013
aqueous nC_{60} , fullerol, polyvinylpyrrolidone (PVP) and citrate stabilized nAg	silicate glass beads (360 μm)	0.36	10 cm	<i>Pseudomonas aeruginosa</i> ATCC 7700 and <i>Bacillus cereus</i> ATCC 14579	in the column for 2 days	1 mM NaCl (pH-N/A)	2.2×10^{-4} m/s	attachment efficiency increased in the presence of biofilm (except for PVP coated nAg)	Xiao and Weisner, 2013
ZnO nanoparticles	quartz sand (510 μm)	0.42	20 cm	<i>Escherichia coli</i>	in the column for 80 h at 25 °C	0.1-5 mM NaCl and 0.05-0.5 mM CaCl_2 (pH 8)	$(4.6-9.3) \times 10^{-5}$ m/s	enhanced nanoparticle retention in the presence of biofilm	Jiang et al. 2013
quantum dots, nano- and micro-sized polystyrene latex particles	763 μm	0.35	8 cm	<i>Pseudomonas aeruginosa</i> ATCC 27853	in the column for 24 h at 37 °C	10 mM KCl (pH 7.2)	6.6×10^{-5} m/s	enhanced nanoparticle retention in the presence of biofilm (attachment efficiency increased in the presence of biofilm); physical straining was an important mechanism for the retention of micron-sized latex particles	Tripathi and Tufenkji, 2012
poly (acrylic acid) stabilized zero valent iron nanoparticles (NZVI)	soda-lime glass spheres (~550 μm)	0.4	14 cm	<i>Pseudomonas aeruginosa</i> PAO1 wild type	in the column for 5 days	1, 25 mM NaCl (pH 7.5)	9.7×10^{-5} m/s	enhanced nanoparticle retention in the presence of biofilm at higher IS (25 mM); the retention was unchanged at lower IS (1 mM)	Learner et al., 2012
fullerene (nC_{60})	quartz sand (417-600 μm)	0.42	20 cm	<i>Escherichia coli</i> BL21	in the column for 80 h at 25 °C	1-25 mM NaCl and 0.1-5 mM CaCl_2 (pH 6.8)	$(4.6-9.3) \times 10^{-5}$ m/s	enhanced nanoparticle retention in the presence of biofilm	Tong et al., 2009

Characterization of Pd-NZVI. The hydrodynamic diameter (z-average reported) and electrophoretic mobility (EPM) were determined using dynamic light scattering (DLS) and laser Doppler electrophoresis (ZetaSizer Nano ZS, Malvern). Measurements were carried out for both the influent suspensions injected into the column, and the effluent suspensions collected after two pore volumes. Both sizing and EPM measurements were done at least in triplicate for 2-4 independent samples per treatment at room temperature ($\sim 22^{\circ}\text{C}$).

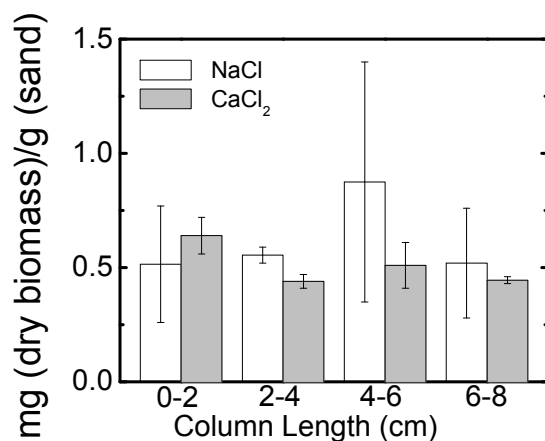


Fig. S1 Biomass along the column length whereby 0-2 cm is the column influent and 6-8 cm is the column effluent after dissecting the column into four segments following equilibration with background electrolyte (10 mM NaCl or CaCl₂). Error bars represent standard deviations of the replicate measurements. The average biomass (average of four segments in Fig. S1) is 0.62 ± 0.17 and 0.51 ± 0.09 mg/g sand, respectively, in 10 mM NaCl and 10 mM CaCl₂ equilibrated column, and the biomass is homogeneously distributed; *i.e.*, an inspection of Fig. S1 does not show spatial biomass variation along the column length. The data presented here is consistent with a previous study where uniform biomass coverage was also observed.²

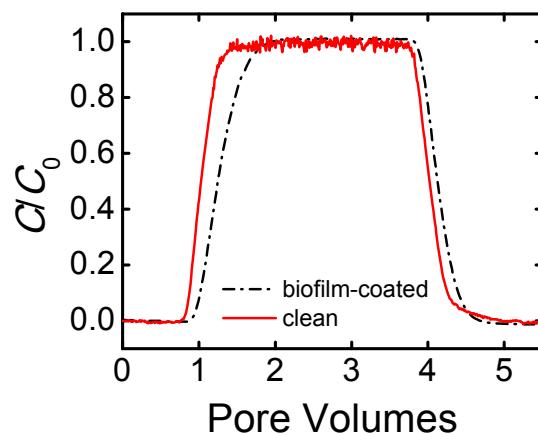


Fig. S2 Tracer (10 mM KNO_3) breakthrough behavior in clean and biofilm-coated sand packed column. The concentration of influent and effluent tracer was monitored using a UV-vis spectrophotometer at 240 nm.

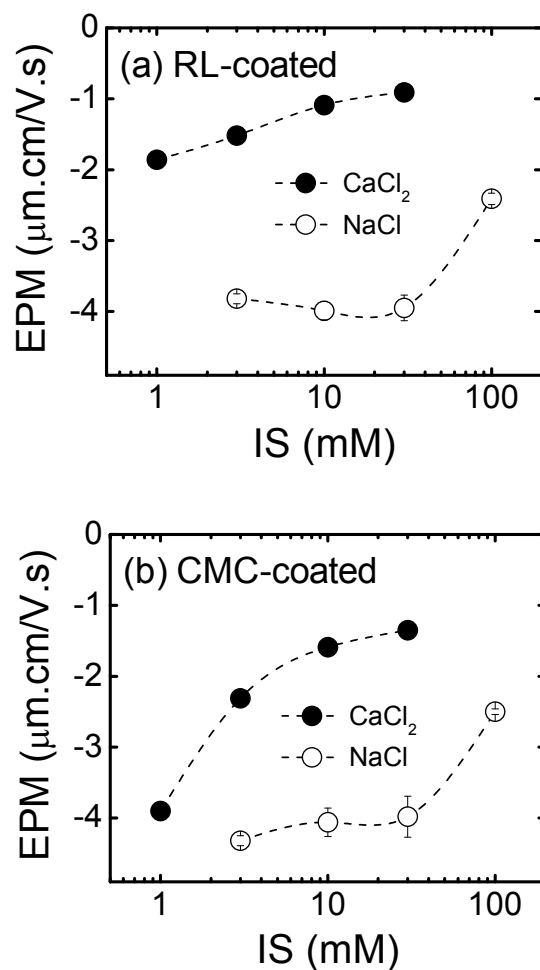


Fig. S3 Measured electrophoretic mobility (EPM) for the influent (a) RL-coated and (b) CMC-coated Pd-NZVI over a range of IS in monovalent (NaCl) and divalent (CaCl_2) salt. Data represents the mean \pm 95 % confidence interval. The dashed lines are included to guide the eye.

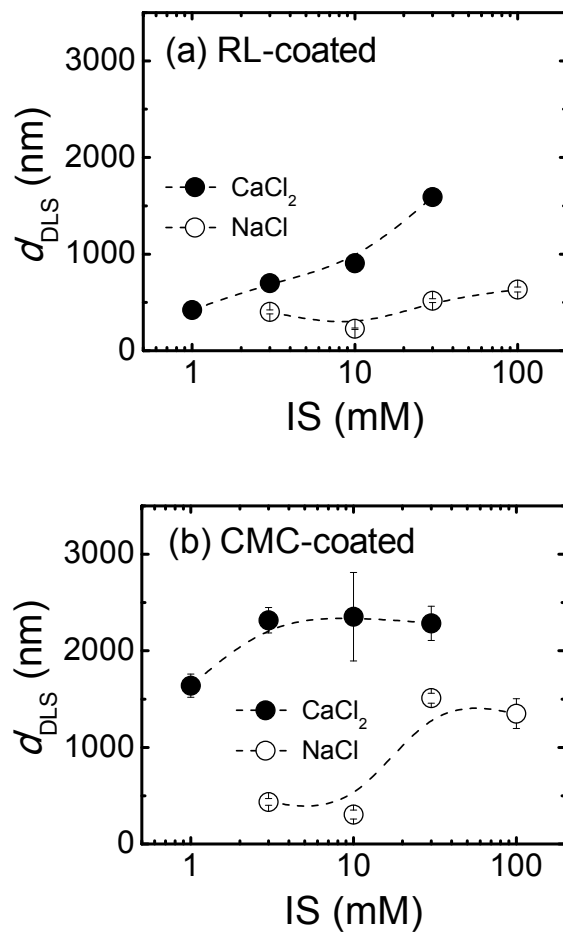


Fig. S4. Hydrodynamic diameter measured using dynamic light scattering (d_{DLS}) for the influent (a) RL-coated and (b) CMC-coated Pd-NZVI over a range of IS in monovalent (NaCl) and divalent (CaCl₂) salt. Data represents the mean \pm 95 % confidence interval. The dashed lines are included to guide the eye.

Table S2. Dynamic light scattering (DLS) measured hydrodynamic diameter of Pd-NZVI injected into the column experiments (influent suspension) and eluted from the column (effluent suspension).

particle	mM IS		Influent	effluent
	(NaCl)	(CaCl ₂)	d_{DLS} (nm)	d_{DLS} (nm)
RL-coated Pd-NZVI				
biofilm-coated sand	3		402 ± 20	371 ± 4
	10		227 ± 8	216 ± 4
	30		518 ± 20	413 ± 16
	100		634 ± 25	437 ± 21
clean sand		1	421 ± 15	564 ± 23
		3	700 ± 35	627 ± 18
		10	906 ± 36	542 ± 17
		30	1590 ± 64	948 ± 73
biofilm-coated sand		1		176 ± 4
		3		315 ± 29
		10		364 ± 26
CMC-coated Pd-NZVI				
biofilm-coated sand	3		435 ± 35	440 ± 12
	10		305 ± 47	328 ± 26
	30		1510 ± 51	1183 ± 71
	100		1350 ± 155	591 ± 107
clean sand		1	1639 ± 121	1035 ± 93
		3	2317 ± 132	1416 ± 99
		10	2353 ± 458	1900 ± 99
		30	2285 ± 177	1424 ± 108
biofilm-coated sand		1		1241 ± 56
		3		2389 ± 244
		30		1012 ± 171

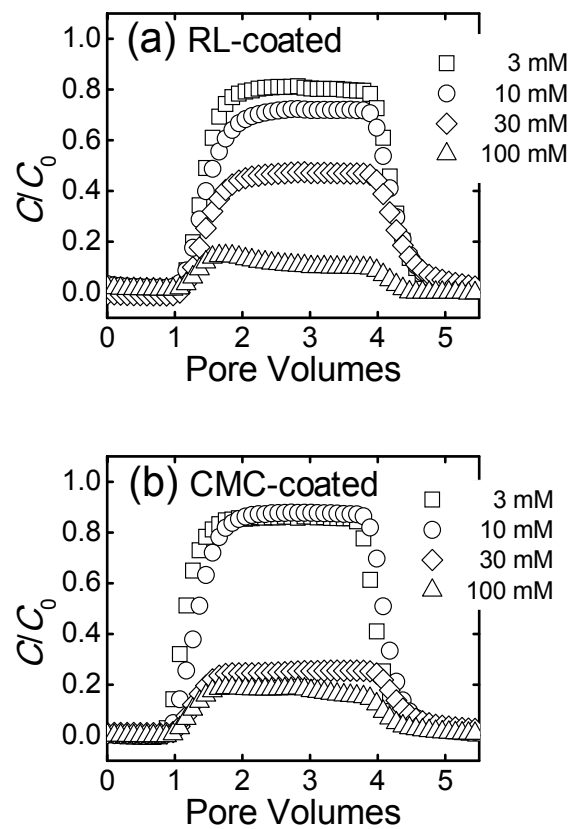


Fig. S5. Measured breakthrough curves at different IS of NaCl in biofilm-coated sand for (a) RL-coated and (b) CMC-coated Pd-NZVI at 0.15 g/L.

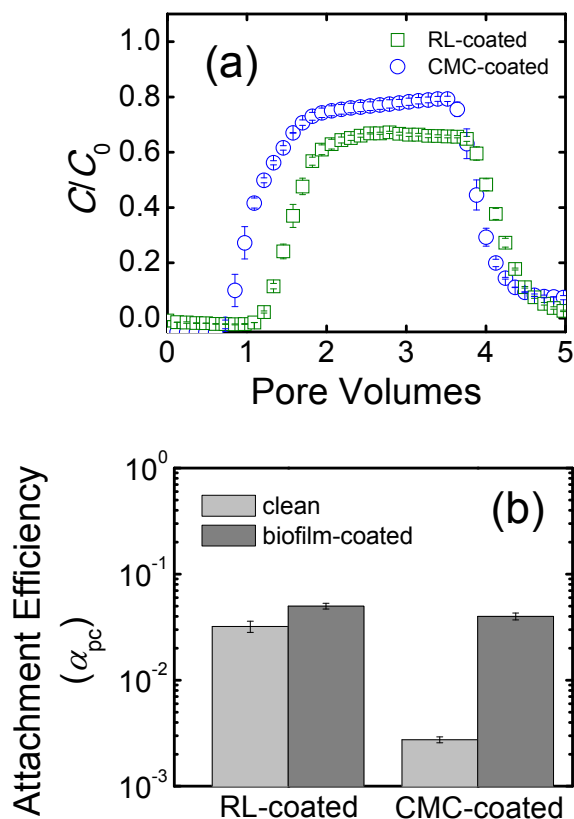


Fig. S6 (a) Measured breakthrough curves in biofilm-coated sand packed column for RL- and CMC-coated Pd-NZVI at 1 g/L (10mM NaCl). (b) Calculated particle-collector attachment efficiency (α_{pc}) for 1 g/L RL- and CMC-coated Pd-NZVI in clean sand and biofilm-coated sand packed column. For comparison, the α_{pc} value in clean sand was adopted from our previous work.¹ [Nanoparticle physicochemical properties are included in Table S3.](#)

Table S3. Physicochemical properties of the Pd-NZVI used in column transport experiments at 1 g/L.

Pd-NZVI (1 g/L)	d_{DLS} (nm)		EPM ($\mu\text{mcm/Vs}$)	
	influent	effluent	influent	effluent
CMC-coated	777 ± 80	843 ± 45	-4.68 ± 0.28	-4.64 ± 0.20
RL-coated	145 ± 15	132 ± 12	-3.97 ± 0.18	-3.94 ± 0.20

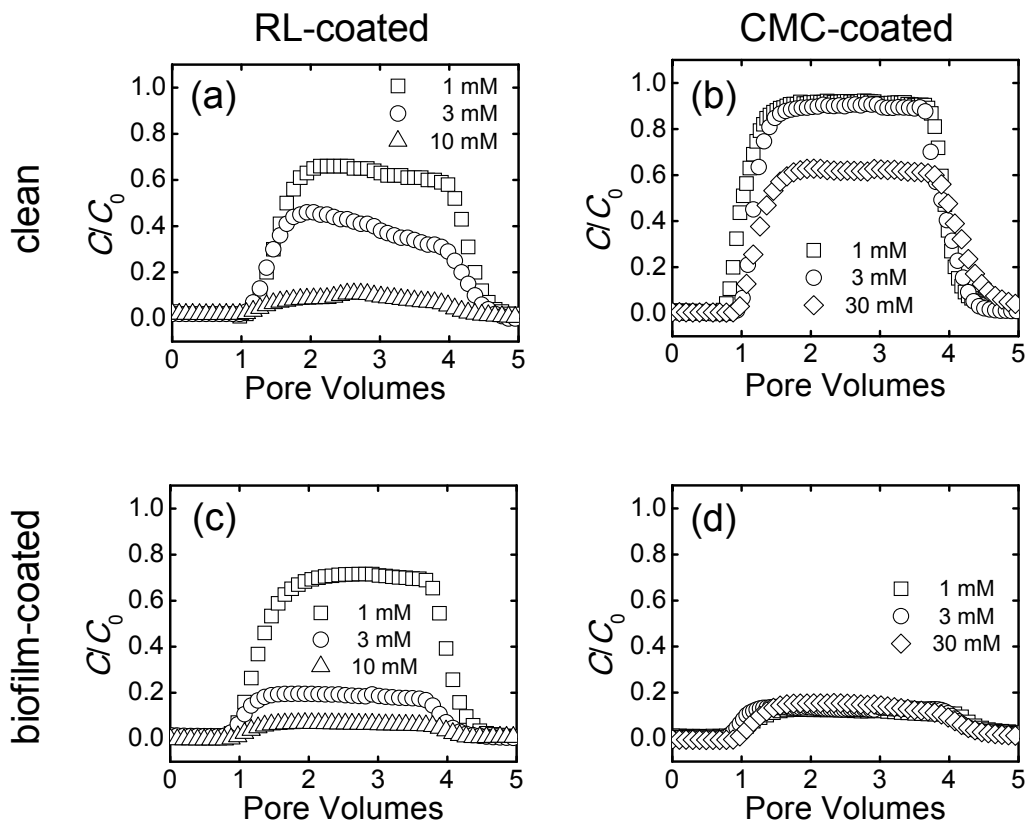


Fig. S7 Measured breakthrough curves at different IS of CaCl₂ in (a, b) clean sand and (c, d) biofilm-coated sand for (a, c) RL-coated and (b, d) CMC-coated Pd-NZVI at 0.15 g/L.

Table S4. Summary of Pd-NZVI elution occurred through the columns packed with either clean or biofilm-coated sand. The particle concentration was 0.15 g/L.

particle	mM IS		elution (C/C_0)	
	(NaCl)	(CaCl ₂)	clean sand	biofilm-coated sand
RL-coated Pd-NZVI	3		0.85 ± 0.00	0.80 ± 0.08
	10		0.86 ± 0.04	0.71 ± 0.03
	30		0.76 ± 0.05	0.47 ± 0.02
	100		0.68 ± 0.02	0.12 ± 0.01
		1	0.62 ± 0.08	0.67 ± 0.05
		3	0.40 ± 0.06	0.19 ± 0.03
		10	0.09 ± 0.03	0.06 ± 0.01
		30	0.01 ± 0.01	<i>n.d.</i>
CMC-coated Pd-NZVI	3		0.93 ± 0.03	0.85 ± 0.07
	10		0.72 ± 0.01	0.86 ± 0.02
	30		0.65 ± 0.03	0.28 ± 0.10
	100		0.39 ± 0.09	0.18 ± 0.01
		1	0.93 ± 0.05	0.15 ± 0.03
		3	0.85 ± 0.02	0.16 ± 0.01
		30	0.65 ± 0.14	0.15 ± 0.08

Note:

Pd-NZVI elution through each column was calculated from the numerical integration of BTCs

The value of elution in clean sand at 3-100 mM NaCl was adopted from our previous work¹

The error bars represent the range of elution occurred in replicate experiments

Pd-NZVI Transport Potential. Semi-quantitative comparison of the transport potential is made via calculated particle-collector attachment efficiency (α_{pc})³:

$$\alpha_{pc} = -\frac{2}{3} \frac{d_c}{(1-\theta)L\eta_0} \ln\left(\frac{C}{C_0}\right) \quad (\text{S1})$$

where d_c is the mean collector diameter, θ is the bed porosity, L is the packed-bed length, and η_0 is the single-collector contact efficiency calculated using the Tufenkji-Elimelech equation⁴ that incorporates three transport mechanisms: (i) transport by diffusion (η_D), (ii) transport by interception (η_I) and (iii) transport by gravity (η_G) ($\eta_0 = \eta_D + \eta_I + \eta_G$).

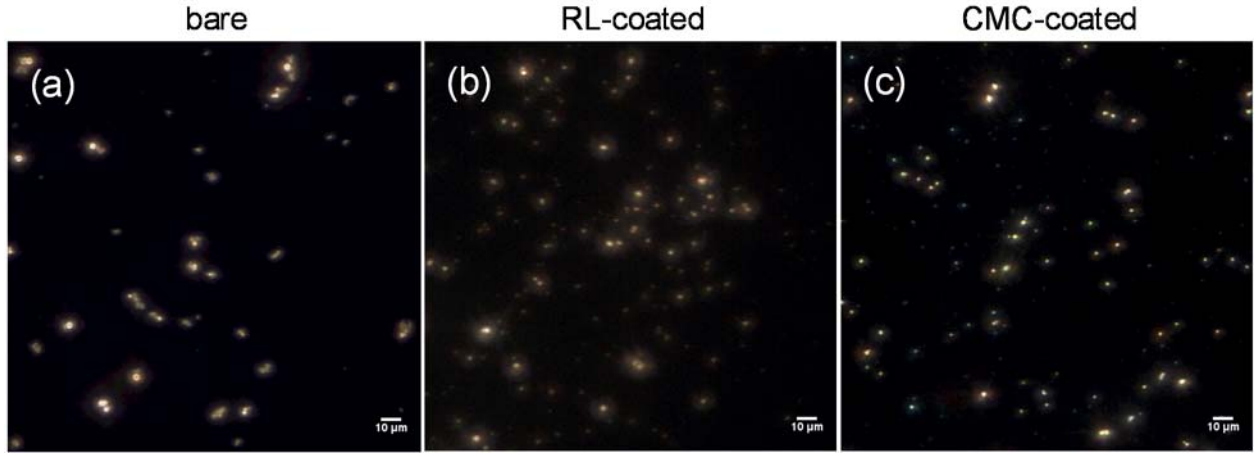


Fig. S8 Hyperspectral imaging for (a) bare, (b) RL-coated and (c) CMC-coated Pd-NZVI obtained with 400× magnification.

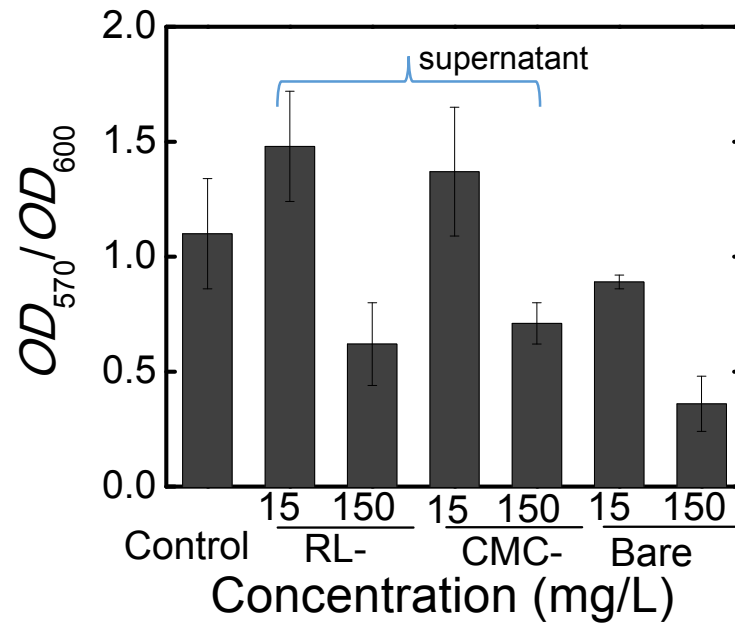


Fig. S9 Growth normalized quantitative estimate of the biofilm formed at the end of growth period (24 hours) measured using crystal violet assay (OD_{570}/OD_{600}).

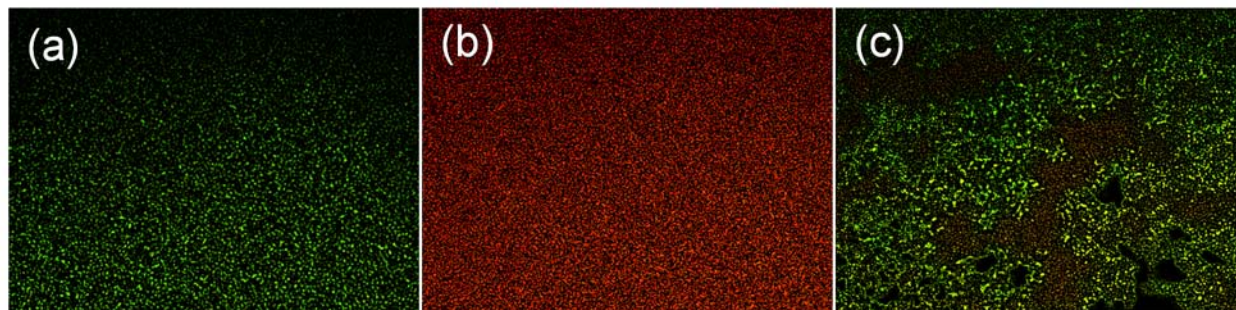


Fig. S10 Representative Live/Dead fluorescence microscopy images of biofilm cells grown on 24-well plate: (a) control (viability ~100 %), (b) 70% ethanol treated control (viability ~ 0 %) and (c) Pd-NZVI exposed (24 h) treatment (viability ~ 63%). At least 30 images acquired per treatment, and analyzed using Image J (ImageJ 1.43m, NIH, USA) to calculate the area pertaining to red (dead) or green (live) cells. The loss in viability was expressed as the ratio of red to total (red + green) area.

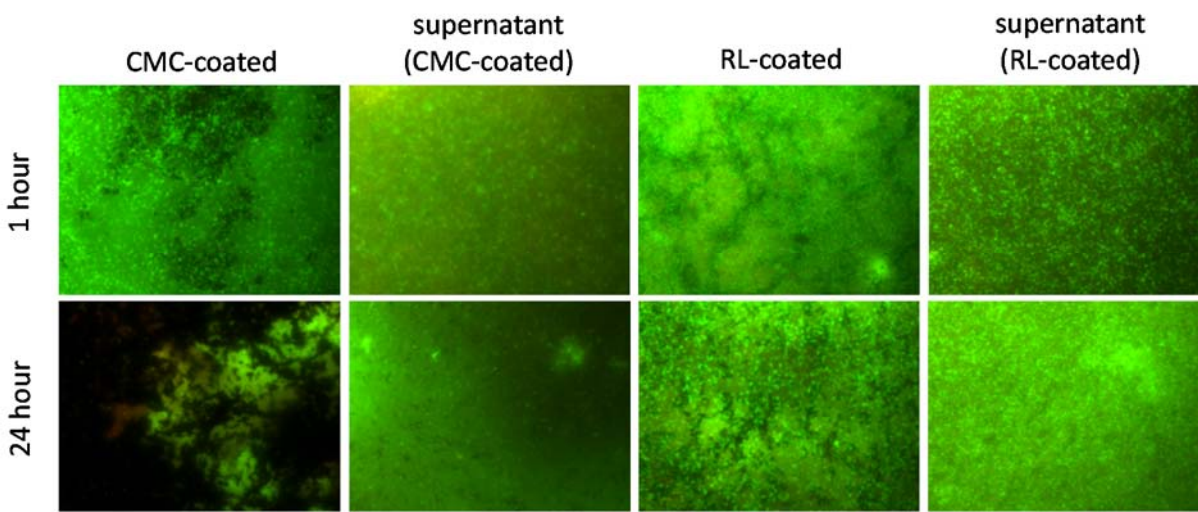


Fig. S11 Representative Live/Dead fluorescence microscopy images of biofilm cells grown on 24-wells plate after 1 or 24 hour exposure with 1 g/L CMC- and RL-coated Pd-NZVI suspension, and with the supernatant (separated using super magnet).

References

1. M. Basnet, C. D. Tommaso, S. Ghoshal and N. Tufenkji, *Water Res.*, 2015, **68**, 354-363.
2. M. R. Mitzel and N. Tufenkji, *Environ. Sci. Technol.*, 2014, DOI: 10.1021/es404598v.
3. K.-M. Yao, M. T. Habibian and C. R. O'Melia, *Environ. Sci. Technol.*, 1971, **5**, 1105-1112.

4. N. Tufenkji and M. Elimelech, *Environ. Sci. Technol.*, 2004, **38**, 529-536.